Assessing the Demand Response Potential of Heat Pumps in All-Electric Buildings Equipped with PV, EV (V2G) and BES to Minimize Energy Costs

Gaona, David ; Vermeer, Wiljan; Chandra Mouli, Gautham Ram; Bauer, Pavol

DOI
10.1109/PEMC51159.2022.9962913

Publication date
2022

Document Version
Final published version

Published in
Proceedings of the 2022 IEEE 20th International Power Electronics and Motion Control Conference (PEMC)

Assessing the Demand Response Potential of Heat Pumps in All-Electric Buildings Equipped with PV, EV (V2G) and BES to Minimize Energy Costs

David Gaona, Wiljan Vermeer*, Gautham Ram Chandra Mouli*, Pavol Bauer*

* Delft University of Technology, 2628 CD Delft, Netherlands (e-mail: W.W.M.Vermeer@tudelft.nl)

2022 IEEE 20th International Power Electronics and Motion Control Conference (PEMC) | 978-1-6654-9681-0/22/$31.00 ©2022 IEEE | DOI: 10.1109/PEMC51159.2022.9962913

Abstract: An integrated energy system consisted of PV panels, EV (electric vehicle), BES (battery energy storage), and a HP (heat pump) coupled with thermal storage tanks (TES) has been studied. The research aimed to minimize the total energy costs by scheduling the optimal power consumption of each device as response to two external signals as part of a demand response program. One of the signals corresponded to a selling electricity price tariff or feed-in tariff (FIT) to account for the ability of the system to sell energy towards the grid. On the other hand, the second signal corresponded to the buying electricity price tariff to account for the system's energy consumption from the grid. This control scheme allowed to determine the optimal energy consumption of the HP and its flexibility potential to shift its load towards times of low electricity prices. It was concluded that the proposed integrated system will produce a 50 % total energy cost reduction while the operation of the HP for one week in winter will reduce the gas consumption in 53 m^3 in a traditional Dutch house.

Keywords— Demand response program, heat pump (HP), thermal energy storage (TES), energy systems optimization, integrated energy systems.

I. Introduction

Following the international climate change agreement, the Netherlands has delimited its road to reduce drastically its greenhouse gases emissions to reach the climate neutrality goal by the second half of the 21st century. To accomplish this, a restructuring of the energy systems into more sustainable forms will be required by distinguishing how the energy is used in four main functions: space heating, industrial process heat, power and light, and transport [1]. Traditionally, the Dutch energy system has relied mainly on natural gas and fossil fuels while a small proportion of renewable energies has been included. It was demonstrated by [2] that only 7% of the total energy produced in the country comes from wind and solar technologies while the remaining corresponded to fossil-fuelled power plants. Fossil systems are characterized by a stable electricity production where the power output can be controlled to match the daily demand. However, this does not occur with renewable energy sources because their intermittent nature results in a fluctuating electricity production causing major problems in the supply-demand balance within the energy market [3]. As more electricity will be produced by using renewable sources, it is important to integrate systems and programs to address such mismatch problem. In this context, different approaches, technologies, and strategies have been investigated to manage the variable renewable electricity from wind and solar. All these tactics have as main characteristic the study of the "flexibility potential" that new energy systems can offer to attenuate these intermittency effects to keep the grid stable. On the demand side, the main approach is to address the problem towards demand response programs (DRP) such that the customer's energy consumption can be modified by using smart technologies that respond to some external signals. Here, the consumer performs his daily activities under an optimized energy scheduling framework that assures the satisfaction of his needs while consuming the least amount of energy at the lowest cost.

A. Energy systems optimization review

Steen, Stadler [4] proposes a MILP model for the design of thermal storage systems (TES) to determine the feasibility of investing in TES in combination with DER. The model describes a linearization of the TES with calculation of thermal losses based on the energy contained in the storage tank and allows the use of heat pumps only for low temperature storage charging. Terlouw, AlSkaif [5] have proposed an optimal demand response model for all-electric residential systems with heat and electricity storage through a battery and an electric vehicle. This model includes surface heating (SH) and domestic hot water (DHW) provision through an ASHP capable of providing both SH and DHW simultaneously. In Wolf [6] a model-based assessment of heat pump flexibility was performed by simulating a pool of heat pumps and creating different thermal load profiles for space heating and domestic hot water. The author states that two different heat pumps, a back-up electric heater, and a DWH storage tank have been used to model the entire system. Hedegaard and Balyk [7] established a model to determine the effects on investment of energy systems incorporating heat pumps with thermal storage in buildings and buffer tanks in a Danish case. This model analyzes individual heat pumps and storage systems to optimize investments and operation, and it incorporates the thermal building dynamics and covers the use of passive heat storage by using the thermal inertia of the building, active heat storage by heating floor systems, and storage tanks for space heating and domestic hot water.

The aim of this research is to assess the flexibility potential of a heat pump for space heating and domestic hot water through an energy cost minimization model of an integrated household considering PV panels, a battery energy storage system (BES), a heat pump (HP), and an electric vehicle in a simulated demand response program driven by variable electricity price signals

B. Contribution of the paper.

This research will intend to provide a model to perform an energy cost minimization to encourage the use of renewable

energy systems to satisfy residential energy demands. By simulating a demand response program, this paper aims to achieve a reduction in the energy consumption for residential heating by determining the optimal operation of a heat pump. In this way, determining how flexible the system becomes when heat pumps and thermal storage systems are included is vital to know the limits of the proposed solution.

The goal of this paper is to to determine the extent of the flexibility achieved in integrated power systems in households, and it can contribute to encourage the inclusion of heat pumps as a flexibility service for future energy systems. From the results of this project, different parties within the energy sector can get insights about the possibilities and benefits of using all-electric systems as a reliable option to minimize the consumer's energy bill.

II. METHODS AND MODELLING

A. Description of the system

The integrated energy system shown in Figure 5 is composed by solar panels (PV), a battery energy storage system (BES), and electric vehicle (EV-V2G) connected to the DC side of a multi-port power converter (MPPC). On the AC side, a heat pump (HP) is connected for building heating/cooling, and at the same time, the heat pump is coupled to a thermal energy storage tank (TES) to provide extra flexibility to the system, satisfy the thermal demand of the building, and reduce the electricity consumption of the heat pump. Additionally, a smart grid operator (SGO) is considered to provide the purchasing and selling electricity price signals under which the system will act as part of the demand respond program. The model incorporates degradation costs of EV and BES due to their charging/discharging cycles to provide a more realistic approach. The BES and EV have a bidirectional operation, meaning that they can absorb and inject energy to the grid if it is needed, providing in this way ancillary services to maintain the stability of the grid.

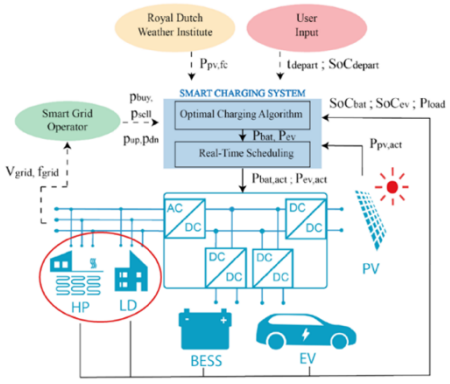

Figure 1: Schematic diagram of the general system

Furthermore, based on the solar irradiation received, it is expected that the PV panels will generate as much power as possible to feed the entire system and reduce the power intake from the grid, and if any excess is present, it will be injected to the grid.

Thermal demand pattern

Residential demand profiles and ambient temperature profiles are required to determine how the system must operate to satisfy these energy requirements, and how much heat loss the building will face. For this specific problem, a typical Dutch house in the city of Delft has been selected. The demands for surface heating (SH) and domestic hot water (DHW) have been obtained from the Applied Natural Science Research (TNO) organization and [8] respectively as seen in figure 2 and 3. The data set provided by TNO corresponds to a study case for year 1987 where the most extreme winter was registered.

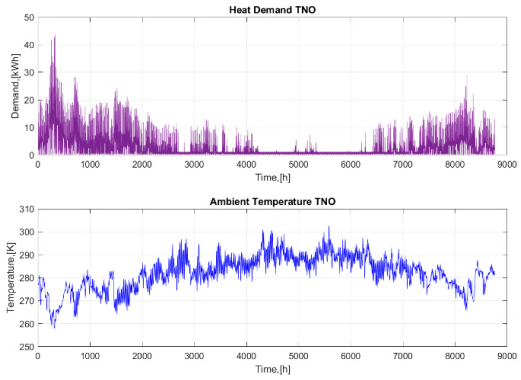

Figure 2: Surface heating demand and ambient temperature, Delft

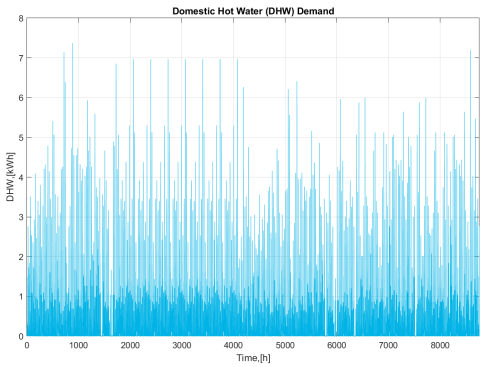

Figure 3: Domestic hot water demand [8]

A correlation between the SH demand expressed in [kW] and the ambient temperature in [K] was obtained such that the model can predict the heat demand by knowing the ambient temperature.

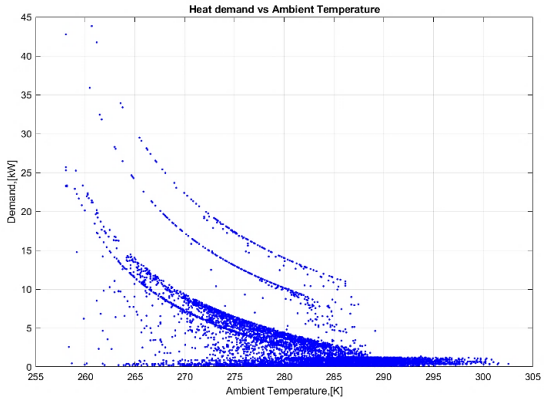

Figure 4: Surface heating demand and ambient temperature relation.

A percentile analysis was conducted to determine the best fitting correlation. It was found that the percentiles 25 (P25) and 35 (P35) have the best fitting correlations. For this project, the percentile 25 correlation has been used to

interpolate the heat demand data considering Delft's average ambient temperature data as expressed in (1).

$$\dot{Q}_{demand,SH} = 4.588 * 10^{12}\ e^{-0.09991 * T_{amb}} \quad (1)$$

B. HP-TES modelling considerations

The heating system is constituted by an air source heat pump (ASHP), two storage tanks (TES) for SH and DHW, and a household. The HP will supply heat for SH and DHW individually to the water tanks to meet the total heating demand of the household. The main state variables will be the water temperature of the SH and DHW tanks (T_{SH}, T_{DHW}), and the temperature of the air inside the building (T_{BUILD}) that must be maintained within desired limits. The COP was estimated by using technical data provided by LG as expressed in (2), and it was considered that the HP provided a minimum water temperature of 35 ˚C, and the building temperature was set to 20˚C as recommended by **[9]**.

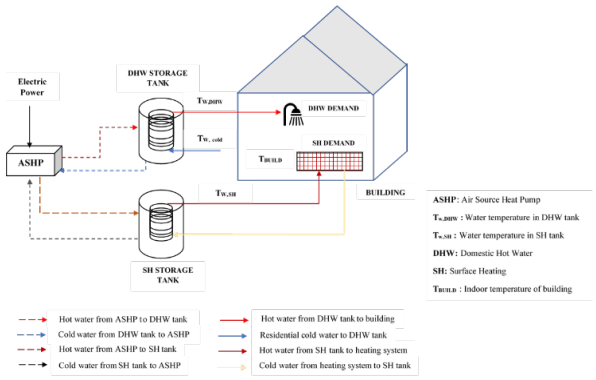

Figure 5: Schematic diagram of the heating system

$$COP_{heating} = a_0 - a_1\,(T_w - T_{amb}) + a_3 (T_w - T_{amb})^2 \quad (2)$$

Table 1: COP model regression coefficients

Coefficient	Value	Unit
a_0	7.8276	-----
a_1	0.1396	K^{-1}
a_2	0.0008	K^{-2}
a_{0c}	5.5146	----
a_{1c}	0.0604	K^{-1}
a_{2c}	-0.0006	K^{-2}

Continuous-time energy balances were performed in each one of the system's components obtaining the corresponding differential equations. However, the approximation of the differential equations was accomplished by applying the forward finite difference method (FFD) to obtain a numerical solution as this is a problem with boundary values. As result, the following equations were obtained:

- Energy balance in the DHW storage tank

$$T_{W,DHW\,(t+1)} = T_{W,DHW\,(t)} + \frac{\dot{Q}_{HP,dhw\,(t)} - \dot{Q}_{build,dhw\,(t)} - \dot{Q}_{loss,DHW\,(t)}}{\rho_w \cdot Cp_w \cdot V_{w,dhw}} \Delta t \quad (3)$$

- Energy balance in the SH storage tank

$$T_{W,SH\,(t+1)} = T_{W,SH\,(t)} + \frac{\dot{Q}_{HP,SH\,(t)} - \dot{Q}_{build,SH\,(t)} - \dot{Q}_{loss,SH\,(t)}}{\rho_w \cdot Cp_w \cdot V_{w,SH}} * \Delta t \quad (4)$$

- Energy balance in the household

$$T_{room\,(t+1)} = T_{room\,(t)} + \frac{\dot{Q}_{build,SH\,(t)} - \dot{Q}_{loss,build\,(t)}}{C_{m\,,build} + (V_{air} \cdot Cp_{air} \cdot \rho_{air})} * \Delta t \quad (5)$$

- HP power consumption

$$P_{HP,SH(t)} = \frac{\dot{Q}_{HP,SH(t)}}{CoP_{SH(t)}} \quad (6)$$

$$P_{HP,DHW(t)} = \frac{\dot{Q}_{HP,DHW(t)}}{CoP_{DHW(t)}} \quad (7)$$

$$P_{HP\,(t)} = P_{HP,SH(t)} + P_{HP,DHW\,(t)} \quad (8)$$

Equation (8) does not mean that the heat pump will operate in SH and DHW mode simultaneously, thus in the optimization algorithm the power consumption has been integrated as a unique variable. Therefore, if the HP is working in SH mode, the $P_{HP,DHW(t)}$ will be equal to zero and vice versa. It must be noted that all the variables will be restricted to upper and lower boundaries by considering technical criteria and recommendations from [9], [5], and[10].

C. Heat storage sizing

The sizes of the WST need to be specified, but as DHW and SH demands are dependent on the number of people and their occupancy behavior, it is difficult to predict the exact demand and related it accurately to the size of a thermal storage device. According to **[11]**, heuristic techniques must be applied to calculate their size and validated models are presented to estimate with appropriate accuracy the storage level needed considering the number of household's inhabitants. The following equations have been applied to size the storage tank's volumes for both demand

$$V_{DHW} = 1.25 \cdot 65 \cdot \left(N_{people}\right)^{0.7} \quad (9)$$

$$V_{SH} = \frac{\dot{Q}_{PEAK} \cdot 2h}{\rho_w \cdot Cp_w \cdot \Delta T} \quad (10)$$

Equations (12) and (13) represent the heat losses in both SH and DHW storage tanks. The surface area of the tanks was calculated by (11). $A_{s,SH}$ and $A_{s,DHW}$ represent the surface areas of the SH and DHW tanks respectively, $T_{w,SH(t)}$ and $T_{w,DHW(t)}$ are the time-dependent water temperatures in the SH and DHW tanks, and $T_{room(t)}$ is the temperature inside the building.

$$A_s = 2\pi R \cdot H + 2\pi R^2 \tag{11}$$

$$\dot{Q}_{loss,SH(t)} = U_{tank} \cdot A_{s,SH} \cdot \left(T_{w,SH(t)} - T_{room(t)}\right) \tag{12}$$

$$\dot{Q}_{loss,DHW(t)} = U_{tank} \cdot A_{s,DHW} \cdot \left(T_{w,DHW(t)} - T_{room(t)}\right) \tag{13}$$

The type of building in this study was a terraced house with a medium insulation level, and it was identified as B-level energy performance building according to [12]. For this research, three types of heat losses have been considered: convection and conduction heat losses through the walls, and heat losses due to natural ventilation. Using information available in [13] and [14] heat losses due to ventilation have been estimated for a typical Dutch terraced house. These losses have been estimated as follows:

$$\dot{Q}_{cond\,(t)} = U_{building} \cdot A_{building} \cdot \left[T_{room(t)} - T_{amb(t)}\right] \tag{14}$$

$$\dot{Q}_{vent\,(t)} = \lambda \cdot V_{building} \cdot ACH \cdot \left[T_{room(t)} - T_{amb(t)}\right] \tag{15}$$

Where the factor λ corresponds to the product of the air's density and its heat capacity at an average temperature between the room and ambient temperatures, and it has units of kWh m^{-3} K^{-1}.

D. Optimization model

The cost minimization can be achieved by reducing the energy intake from the grid, selling the excess of electricity to the grid, or using as much as possible of the generated PV power. The SGO will provide the electricity price signals for both buying and selling electricity. The model will try to find the optimal points where the operational costs are minimized according to the following objective function:

$$\min_{C_{PV}, C_{EV}, C_{BES,}\, C_{grid}} C_{total} = \min\left(C_{PV} + C_{BES} + C_{EV} + C_{grid}\right) \tag{16}$$

where C_{PV} corresponds to the installation and investment costs of the PV panels, C_{BES}, and C_{EV} correspond to the degradation costs of the BES and the EV due to their operation, and C_{grid} corresponds to the operational costs of the grid due to the power exchanges of the studied system with the grid. In this way, a non-linear programming (NLP) optimization problem was obtained. The degradation costs of the stationary battery have been determined by considering a loss of value per kWh (€/kWh) and a loss of capacity during their lifetime operation as proposed in [15]. The operational costs C_{BES} would be equal to the difference between a new and a degraded battery, and they have been calculated using the following equations:

$$V_{BES}^{2nd} = V_{BES}^{1st} \cdot \frac{E_{BES\,max} - \Delta E_{BES,tot}}{E_{BES\,max}} \tag{17}$$

$$C_{BES} = V_{BES}^{1st} \cdot E_{BES\,max} - V_{BES}^{2nd} \cdot \left(E_{BES\,max} - \Delta E_{BES,tot}\right) \tag{18}$$

where V_{BES}^{2nd} corresponds to the second-life value of the battery, $\Delta E_{BES,tot}$ represents the degraded capacity of the battery, $E_{BES\,max}$ is the initial capacity, and V_{BES}^{1st} equals to the initial value of the battery. The degradations costs related to the EV has followed the same reasoning as for the BES and are given in Equation (19)

$$C_{EV} = \left(V_{BES}^{1st} - V_{BES}^{2nd}\right) \cdot \frac{\Delta E_{EV,tot}}{0.2\, E_{EV\,max}} \cdot \left(E_{EV\,max} - \Delta E_{EV,tot}\right) \tag{19}$$

According to [16], when the battery's power for charging or discharging is mathematically captured in a unique variable (P_{BES}), simultaneous charging/discharging of the battery is avoided. Besides, the optimization model recognizes that a simultaneous operation is not optimal for cost minimization, and it will intend to find points where charging and discharging occurs separately. Hence, the following equations have been used to model the charging/discharging operation of the battery, and the energy stored by it:

$$P_{BES(t)} = n_{ch} \cdot P_{BES\,(t)}^{pos} - \frac{1}{n_{dis}} P_{BES\,(t)}^{neg} \tag{20}$$

$$P_{BES\,(t)}^{pos} \leq P_{BES}^{max} \tag{21}$$

$$P_{BES\,(t)}^{neg} \leq P_{BES}^{max} \tag{22}$$

$$E_{BES\,(t)} = E_{BES\,(t-1)} + P_{BES\,(t)} \cdot \Delta t \tag{23}$$

The energy stored by the battery at t=1 and t=t_{final} have been fixed to have a fair comparison in terms of energy/cost. The values of the parameters in equations (18) to (23) are displayed in Table 2.

Table 2: Parameter values for BES degradation costs.

Parameter	Value	Units
V_{BES}^{1st}	500	€
V_{BES}^{2nd}	250	€
η_{ch}	0.96	-----
η_{disch}	0.96	-----
$E_{BES,ini}$	5	kWh

The state of charge (SOC) of the battery can be calculated as the ratio of the energy stored at time step *t* to the actual limit capacity at the same time step.

$$SoC_{BES\,(t)} = \frac{E_{BES\,(t)}}{E_{BES,limit\,(t)}} \tag{24}$$

$$E_{BES,limit\,(t)} = E_{BES\,limit\,(t-1)} - \Delta E_{BES(t)} \tag{25}$$

The capacity lost $\Delta E_{BES(t)}$ has been calculated using a Li-ion degradation model developed by [17] where the behavior of a single cell has been studied. This model investigates the effects of temperature, current rate, and the ampere-hours processed in the degradation of the cell, however, as the

model considers only one cell, the power and voltage of the battery must be scaled down to the voltage and current of one single cell. To do this, the model in [18] is used to establish the relationship between the open circuit voltage (OCV) and the SOC of a battery, as shown in equation (26). For this study, it has been assumed that the battery is composed of $N_{BES}^{parallel}$ x N_{BES}^{series} cells to have an OCV of 425 V at full capacity. This way both the OCV(t) as a function of the SOC(t) and the current of a single cell can be calculated as follows:

$$OCV_{BES\,(t)} = N_{BES}^{series} \text{ x } \left(a_1 \cdot e^{b_1 \cdot SoC(t)} + a_2 \cdot e^{b_2 \cdot SoC(t)} + a_3 \cdot SoC_{(t)}^2\right) \quad (26)$$

$$i_{BES}^{cell} = \frac{1000 \cdot P_{BES\,(t)}}{N_{BES}^{parallel} \cdot OCV_{(t)}} \quad (27)$$

The parameters for the BES and EV models to determine the OCV and the capacity lost are summarized in the Table 3.

Table 3: : OCV and aging parameters for BES and EV

Parameter	Description	Value
$\boldsymbol{a_1}$	OCV parameters	3.679
$\boldsymbol{a_2}$		-0.2528
$\boldsymbol{a_3}$		0.9836
$\boldsymbol{b_1}$		-0.1101
$\boldsymbol{b_2}$		-6.829
$\boldsymbol{c_1}$	Aging parameters	0.0008
$\boldsymbol{c_2}$		0.39
$\boldsymbol{N_{BES}^{parallel}}$	Number of cells in parallel in BES	18
$\boldsymbol{N_{BES}^{series}}$	Number of cells in series in BES	100
$\boldsymbol{N_{EV}^{parallel}}$	Number of cells in parallel in EV	145
$\boldsymbol{N_{EV}^{series}}$	Number of cells in series in EV	100

Next, the capacity's degradation of the battery at any time step, and the total capacity lost has been calculated using the following equations:

$$E_{BES\,limit\,(t=1)} = E_{BES,max} \quad (28)$$

s

$$E_{BES\,(t)} \leq E_{BES\,limit(t)} \quad (29)$$

$$\Delta E_{BES\,(t)} = \left(c_1 \cdot e^{c_2 \cdot |i_{BES}^{cell}(t)|} \cdot |i_{BES\,(t)}^{cell}| \Delta t\right) \cdot \frac{E_{BES,max}}{100} \quad (26)$$

$$\Delta E_{BES,tot} = \sum_{0}^{T} \Delta E_{BES(t)} \quad (27)$$

The degradation of the EV battery has been determined in the same way as for the stationary BES, but it has been assumed that the EV is not available between the times the EV departs from and arrives to the building.

The power consumed during driving is captured in the variable $P_{drive\,(t)}$ for all the time the EV is not in the building. Furthermore, it can be established that the EV needs a minimum amount of charge at the departure time to ensure the EV has enough energy when leaving the building. As in the stationary BES, the EV cannot be charged and discharged at the same time, for the same principle of capturing the EV battery's (dis)charging in a unique variable has been applied. All these considerations have been modelled in the following equations:

$$P_{drive(t)} = \frac{15\ kWh}{100\ km} \cdot \frac{d_{round\ trip}}{\Delta t * N_{steps}^{non\ av}} \quad (28)$$

$$P_{EV(t)} = EV_{av(t)} \cdot \left(n_{ch} \cdot P_{EV\,(t)}^{pos} - \frac{1}{n_{dis}} P_{EV\,(t)}^{neg}\right) \quad (29)$$

$$P_{EV\,(t)}^{pos} \leq P_{EV}^{max} \quad (30)$$

$$P_{EV\,(t)}^{neg} \leq P_{EV}^{max} \quad (31)$$

$$E_{EV\,(t)} = E_{EV\,(t-1)} + \left[\left(P_{EV\,(t)} - P_{drive(t)}\right) \cdot \Delta t\right] \quad \forall t, t \leq t_{depart}\ \&\ t > t_{arrive} \quad (32)$$

$$E_{EV\,(t=1)} = E_{EV,ini} \quad (33)$$

$$E_{EV\,(t=t_{depart})} \geq E_{EV,depart} \quad (34)$$

The SoC of the EV battery can be determined in the same way as for the stationary BES considering the degradation of its capacity during the charging/discharging cycles. Equations (36) to (38) were used to calculate the SoC of the EV.

As PV is a renewable energy source, normally its operational costs are assumed to be zero, but in this research the model has contemplated the investment and installation costs of the photovoltaic system.

$$C_{PV} = \sum_{t=1}^{T} \lambda_{PV} \cdot P_{PV(t)} \cdot \Delta t \quad (35)$$

where $P_{PV(t)}$ represents the power production from the panels, λ_{PV} is the LCOE (levelized cost of energy) of the panels, and Δt is the step time of the optimization. For the system represented in figure 1, two power balances in the multi-port power converter have been developed for simplicity of the modelling. The first one comprehends all the elements connected to the DC side of it (PV, BES, and EV), while the second corresponds to all the elements on the AC side (grid, load, heat pump). Depending on the sign, the variables can represent a power output or input, influencing the direction of the balance. The following equations have been used to calculate these power flows:

$$P_{inv(t)} = P_{PV(t)} - P_{EV\,(t)} - P_{BES(t)} \quad (36)$$

$$P_{grid\,(t)} = P_{inv(t)} - P_{load\,(t)} - P_{HP(t)} \quad (37)$$

$$P_{grid(t)} = n_{cable} \cdot P_{grid\,(t)}^{pos} - \frac{1}{n_{cable}} P_{grid\,(t)}^{neg} \quad (38)$$

$$C_{grid} = \sum_{t=1}^{T} P^{neg}_{grid\,(t)} \cdot \lambda_{buy(t)} \cdot \Delta t - P^{pos}_{grid\,(t)} \cdot \lambda_{sell(t)} \cdot \Delta t \qquad (39)$$

$$P^{neg}_{grid\,(t)} \leq P^{max}_{grid} \quad ; \quad P^{pos}_{grid\,(t)} \leq P^{max}_{grid} \qquad (40)$$

where $P_{inv(t)}$ is the total power balance on the DC side, $P_{EV(t)}$ and $P_{BES(t)}$ represents the power consumption or injection of the EV and BES respectively, $P_{grid(t)}$ corresponds to the power consumption or injection to the grid, $P_{load(t)}$ is the load of the electric appliances of the building, and $P_{HP(t)}$ is the power consumption of the HP for SH or DHW. As the system can use or inject energy into the grid, a distinction between the two events have been considered. A positive grid power represents injection of power on the grid at the corresponding selling price $\lambda_{sell(t)}$, while a negative grid power holds for the power intake from the grid at the buying price $\lambda_{buy(t)}$. The cable's transmission efficiency has been included to account for transmission losses. Besides, to guarantee the grid's stability, the power intake and injection cannot exceed the maximum allowed limit the grid can offer, so capacity constrains have been added. Therefore, the cost imposed on the grid due to these interactions with the system has been calculated using the following equations:

III. RESULTS

These results were obtained by optimizing the operation of the system during 5 days in winter under a demand response program based on two electricity price signals taken from[19]. Additionally, the selling electricity price was halved to ascertain its effect on the behavior and operational costs of the system, for two scenarios were studied.

A. HP operation behavior

Based on the electricity price signals, the cost minimization occurs when the devices operate at the lowest prices. Figure 6 displays the behavior of the heat pump during winter season, and it does not operate at times where electricity prices are the highest while it shifts its power consumption to the lowest prices to fully charge the SH tank.

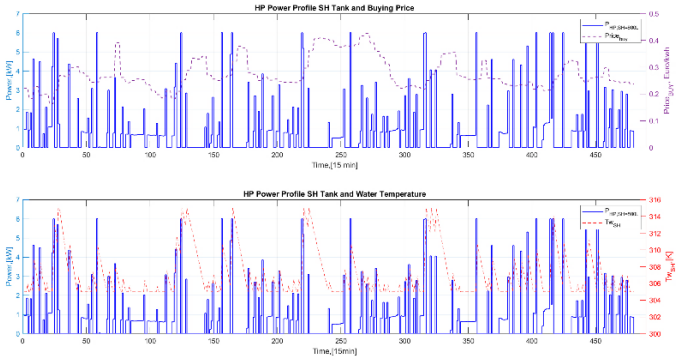

Figure 6: Heat pump operation behavior on price signal

There are times where the heat pump operates at high prices, but it does it at a minimum capacity to keep the SH tank at the lower boundary temperature. This has to do with the fact the model determines that during these times it is not necessary nor cost effective to fully charge the tank because the prices are relatively high, but a minimum amount of energy is still required to keep the thermal comfort of the building.

B. PV-EV-BES-HP system operation

1) High selling price case

Figure 7 shows the optimized power profiles of the different components of the system for the high selling price case. The simulation was carried out for five days, but for the purpose of appreciation only two days are displayed. The behavior of the system has been split into two parts. The top graph represents the power profiles of the components connected to the DC side of the inverter. The bottom graph corresponds to the AC side of the power converter where the grid, the building's load, and the heat pump are connected. It can be seen there is limited interaction between the BES-EV with the HP and the load of the building (see orange circles). Part of the discharged energy is consumed by the loads, and the excess is sold to the grid. This is result of having high FIT because the minimization strategy is more cost effective when the discharged energy is sold instead of being used for self-consumption of the system. On the PV production side, PV electricity was used mainly to charge the battery at times of not too high prices. Nevertheless, most of the time the system prefers to sell PV energy at the highest FIT to minimize the costs even further (see light blue circle).Therefore, PV self-consumption is not performed.

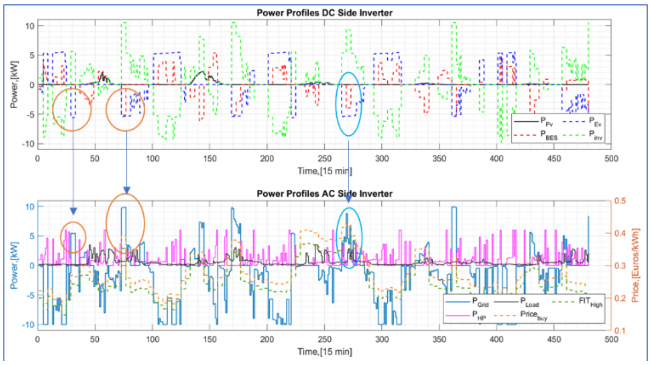

Figure 7: System power profiles for high selling prices

2) Halved selling price case

When the FIT is halved, no selling of energy towards the grid occurs, so the only way for the system to minimize the operational costs is to enhance self-consumption and reduce the energy intake from the grid. The battery and the EV regulate its energy consumption by decreasing the time needed for charging (see orange circles). Besides, the cycles for charging and discharging are decreased, thus the energy is stored for longer periods. On the other hand, the discharging process is done gradually to feed the load and the HP. In the halved FIT, self-consumption is enhanced to minimize the energy costs because there is no injection of energy towards the grid, thus no revenues are obtained. Consequently, the operational strategy of the system has changed towards reducing the energy intake from the grid by using the BES and EV stored energy. This confirms the hypothesis stated at the beginning that decreasing the FIT will enhance self-consumption and reduce the power exchanges with the grid.

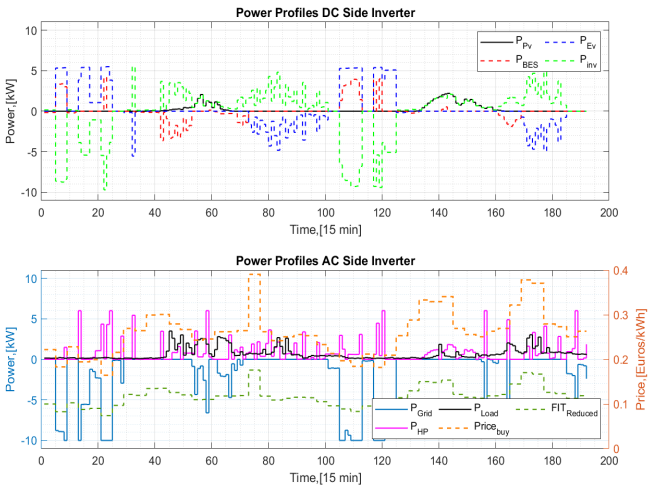

Figure 8: System power profiles for halved selling prices (2 days)

3) Uncontrolled system operation case

Under an uncontrolled scheme where no optimization is performed, the energy consumption takes place at low and high prices. Furthermore, the battery charges using the PV energy available, while the excess is fed mainly to the load and the HP. The discharge of the BES in the evening is used by the load and the HP. Besides, the charge and discharge cycles of the battery are considerably lower than in the optimized cases. Additionally, the HP power profile is continuous because it is used to directly satisfy the heat demand of the building, so its operation scheme changes radically when compared to the optimized cases. This is depicted in the following figure.

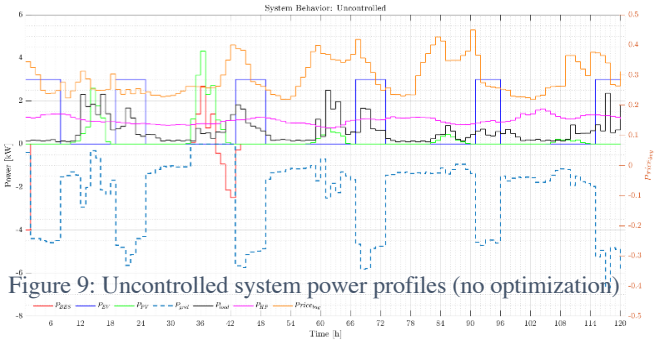

Figure 9: Uncontrolled system power profiles (no optimization)

IV. CONCLUSIONS

The results of the optimization for winter evidenced that high costs reduction could be achieved with the proposed system. It was demonstrated that the FIT signal had a significant influence on the system's cost minimization strategy. A high FIT resulted in a cost minimization through selling high amounts of energy to the grid while with the reduced FIT the minimization was performed by enhancing self-consumption of the PV produced energy and by using the energy stored in the BES/EV. During winter, the minimized costs between the high and reduced FIT cases differed approximately by 10%. In average, the optimization resulted in a minimized cost of 8.58 €/day. By assuming that this cost would be the same per each day of the whole season, this would represent a total energy cost of 755 €. When compared to a system where demand response is not performed, the system costs rose to 17.04 €/day, meaning a seasonal energy cost of 1500 €. Therefore, it can be concluded that during winter the proposed system could generate around 50% energy cost reduction when acting under a demand response program. The minimized costs were also compared to a non-optimized case where no minimization was performed. The results are showed in the following tables.

Table 4: Optimized (high FIT) and Non-Optimized System's cost comparison

Non-Optimized											Δ TOC
V_{SH} L	HP kWh	Grid Drawn kwh	Grid Fed kWh	Grid Expenses €	Grid Revenues €	Grid Cost €	PV cost €	BES Cost €	EV Cost €	TOC €	
----	118.40	280.79	0	82.72	0	82.72	0.418	1.40	0.67	85.21	
Optimized Normal FIT											- 49.63 %
V_{SH} L	HP kWh	Grid Drawn kwh	Grid Fed kWh	Grid Expenses €	Grid Revenues €	Grid Cost €	PV cost €	BES Cost €	EV Cost €	Min. TOC €	
800	118.13	297.84	97.60	68.48	29.90	38.58	0.418	1.73	2.19	42.92	

*The results correspond to an operation for 5 days.

Table 5: Optimized (halved FIT) and Non-Optimized System's cost comparison

Non-Optimized											Δ TOC
V_{SH} L	HP kWh	Grid Drawn kwh	Grid Fed kWh	Grid Expenses €	Grid Revenues €	Grid Cost €	PV cost €	BES Cost €	EV Cost €	TOC €	
----	118.40	280.79	0	82.72	0	82.72	0.418	1.40	0.67	85.21	
Optimized Reduced FIT											-44.54 %
V_{SH} L	HP kWh	Grid Drawn kwh	Grid Fed kWh	Grid Expenses €	Grid Revenues €	Grid Cost €	PV cost €	BES Cost €	EV Cost €	Min. TOC €	
800	117.65	201.99	2.23	44.61	0.24	44.37	0.418	0.96	1.51	47.26	

*The results correspond to an operation for 5 days.

V. ACKNOWLEDGEMENTS

This project was funded by TKI Urban Energy as part of the FLEXgrid project from Delft University of Technology.

VII. REFERENCES

[1] Ministry of Economic Affairs, *Energy Report: Transition to Sustainable Energy*, T. Designers, Editor. 2016, Ministry of Economic Affairs: Netherlands. p. 12.

[2] Kreijkes, M., *Looking under the hood of the Dutch Energy System*, T.J.D. Sherwood, Editor. 2017, Clingendael International Energy Program, CIEP: The Hague. p. 1-35.

[3] Kosmadakis, G., S. Karellas, and E. Kakaras, *Renewable and conventional electricity generation systems: Technologies and diversity of energy systems*, in *Renewable Energy Governance*. 2013, Springer. p. 9-30.

[4] Steen, D., et al., *Modeling of thermal storage systems in MILP distributed energy resource models*. Applied Energy, 2015. **137**: p. 782-792.

[5] Terlouw, T., et al., *Optimal energy management in all-electric residential energy systems with heat and electricity storage*. Applied Energy, 2019. **254**: p. 113580.

[6] Wolf, T., *Model-based Assesment of Heat Pump Flexibility*, in *Teknisk- naturvetenskaplig fakultet*. 2016, Uppsala Universitet: Uppsala. p. 1-76.

[7] Hedegaard, K. and O. Balyk, *Energy system investment model incorporating heat pumps with thermal storage in buildings and buffer tanks*. Energy, 2013. **63**: p. 356-365.

[8] Edwards, S., I. Beausoleil-Morrison, and A. Laperrière, *Representative hot water draw profiles at high temporal resolution for simulating the performance of solar thermal systems*. Solar Energy, 2015. **111**: p. 43-52.

[9] ISO, I.O.f.S., *Energy Performance of Buildings — Calculation of Energy Use for Space Heating and Cooling*. 2008, ISO: Switzerland. p. 162.

[10] Renaldi, R., A. Kiprakis, and D. Friedrich, *An optimisation framework for thermal energy storage integration in a residential heat pump heating system*. Applied energy, 2017. **186**: p. 520-529.

[11] Fischer, D., et al., *Impact of PV and variable prices on optimal system sizing for heat pumps and thermal storage*. Energy and Buildings, 2016. **128**: p. 723-733.
[12] Mudgal, S., et al., *Energy performance certificates in buildings and their impact on transaction prices and rents in selected EU countries*. European Commission (DG Energy), Paris, 2013.
[13] Terlouw, T., T. AlSkaif, and W. van Sark. *Optimal Energy Management of All-electric Residential Energy Systems in the Netherlands*. in *2019 IEEE Milan PowerTech*. 2019. IEEE.
[14] Nash, S., *Impact of mechanical ventilation systems on the indoor-air quality in highly energy-efficient houses*, in *IVEM, Center for Energy and Environmental Studies*. 2013, University of Groningen: The Netherlands.
[15] Kelly, K., et al., *Battery Ownership Model-Medium Duty HEV Battery Leasing & Standardization*. 2015, National Renewable Energy Lab.(NREL), Golden, CO (United States).
[16] Garifi, K., et al., *Control of Energy Storage in Home Energy Management Systems: Non-Simultaneous Charging and Discharging Guarantees*. arXiv preprint arXiv:1805.00100, 2018.
[17] Wang, J., et al., *Degradation of lithium ion batteries employing graphite negatives and nickel–cobalt–manganese oxide+ spinel manganese oxide positives: Part 1, aging mechanisms and life estimation*. Journal of Power Sources, 2014. **269**: p. 937-948.
[18] Baccouche, I., et al., *Improved OCV model of a Li-ion NMC battery for online SOC estimation using the extended Kalman filter*. Energies, 2017. **10**(6): p. 764.
[19] Epexspot. *Market Data*. 2020 [cited 2020 07/04]; Available from: https://www.epexspot.com/en/market-data.